OUTLINE OF POLYNEUTRON THEORY

John C. Fisher
600 Arbol Verde, Carpinteria, CA 93013
jcfisher@fisherstone.com

Abstract

I suggest that neutron clusters of sufficient size are bound and stable against strong decay; and that they can react with ordinary nuclei by transferring neutrons to them, accepting neutrons from them, and binding with them to form composite nuclei. Implications of this enlarged scope of nuclear physics are explored, including a chain reaction with nuclear fuel ^{2}H that produces energy, ^{4}He, ^{3}H, and a wide range of nuclear transmutations. Natural explanations emerge for these and other nuclear phenomena for which evidence has been accumulating over the past two decades.

1. Introduction

Over the past two decades many room-temperature experiments have demonstrated nuclear phenomena that lie outside the purview of present nuclear theory. These include generation of energy in amounts not attributable to non-nuclear sources, production of helium and tritium, generation of high energy alpha particles, and transmutations of ordinary nuclei. Here I propose that massive neutron isotopes, or polyneutrons, are key reactants in this new family of nuclear phenomena.

One widely studied experimental system consists of a glass-walled electrolysis cell containing a palladium or nickel cathode, a platinum anode, and an electrolyte of LiOD, Li_2SO_4 or D_2SO_4 dissolved in D_2O or H_2O. Beginning with the pioneering work of Fleischmann, Pons and Hawkins [2] this system has provided evidence for the generation of energy in excess of amounts that are explicable by electrochemical Processes [10,12] and for production of substantial amounts of ^{4}He [11]. Small amounts of ^{3}H have been observed [19]. Energetic charged particles have been observed by means of detectors immersed in the electrolyte [13,14] and in the vapor over the electrolyte [15]. The review prepared by Storms [18] provides a broad overview of this research. A different experimental system employs flow of deuterium through a thin layer of target element on the surface of a palladium/CaO foil. Transmutations of a number of target elements have been observed [5,6].

In seeking explanations for the foregoing observations we can first rule out deuterium fusion as a contributor because the required reaction products are not observed. Theory rules it out as well because at room temperature there is insufficient thermal energy to overcome the coulomb barrier. Indeed the coulomb barrier rules out every low-temperature nuclear reaction between charged particles, leaving only neutral particles as possible mediators. Neutrons play this role in the commercial reactors that provide energy for electric power generation and ship propulsion, but neutrons cannot be mediators in electrolysis experiments because searches show that they are not present in sufficient numbers. Neutral particles of a different kind are required. Here I explore the possibility that they are polyneutrons.

Polyneutrons can be understood as liquid droplets of neutrons, just as ordinary nuclei have been understood as mixed droplets of neutrons and protons. I propose that they are key reactants

1

in a new family of nuclear phenomena. Based on evidence obtained from particle showers recorded on detector chips exposed to the vapor from electrolysis cells, supplemented by evidence from transmutations and from tritium generation, many of their properties have been deduced and many of their reactions with ordinary nuclei have been quantified.

It emerges that the polyneutrons typically encountered in shower and transmutation experiments contain hundreds of neutrons. They are held together by binding energies of about 7 MeV per neutron, nearly half as strongly as nucleons are bound in ordinary nuclei. A portion of the binding energy is associated with collective pairing of neutrons having opposite spins and momenta, in analogy with electron pairing in superconductors.

Polyneutrons are highly reactive with ordinary nuclei, able to exchange neutrons with them and to catalyze their beta decay. They are beta unstable and transform to massive hydrogen nuclei in which a proton shares the nuclear symmetry of the parent polyneutron. Subsequent beta decays generate polyneutron-derived isotopes of helium and lithium and boron and so on until rising coulomb energy prevents further beta decay. Alpha particle emission then remains the favored decay channel. Exceptionally a rare alpha decay releases a free polyneutron that can ignite a chain reaction in an appropriate environment. The chain reaction may die out, or it may continue at a bounded rate depending on environmental factors.

Polyneutrons can form strongly bound composites with some ordinary nuclei. The composites are stable against beta decay and against flow of neutrons between the polyneutron and the ordinary nucleus. Their decay channels are coordinated double beta and alpha decays of the polyneutron component. Such decays play important roles in shower and transmutation experiments.

2. The theory

The theory is based on three assumptions:

1. Polyneutrons containing six or more neutrons are bound.
2. Polyneutrons undergo beta decay with unchanged nuclear symmetry.
3. Polyneutrons and their decay products obey the laws of nuclear physics.

I employ notation in which ^{A}n is a polyneutron containing A neutrons, and in which ^{A}H$_p$ is a cluster of A−1 neutrons and 1 proton that has the same nuclear symmetry (isospin) as ^{A}n, the same nuclear interaction energy as ^{A}n, and the same excitation spectrum as ^{A}n. The subscript p on ^{A}H$_p$ is a reminder that its nuclear symmetry is identical with that for the polyneutron ^{A}n. Similarly ^{A}He$_p$ is a cluster of A−2 neutrons and 2 protons, and so on. I write $\Delta(^A$n$)$, $\Delta(^A$H$_p)$, $\Delta(^A$He$_p)$, … for their mass excesses in MeV. The mass excesses $\Delta(^A$H$_p)$, $\Delta(^A$He$_p)$, … differ from $\Delta(^A$n$)$ only by the mass difference $\Delta(^1$H$) - \Delta($n$) = -0.782$ MeV per proton and by the coulomb energy of multiple protons.

The challenge to theory is to find numerical values for these mass excesses that can account for the observations of energy, helium, tritium, energetic particles, transmutations, particle showers, and other new low-temperature nuclear phenomena.

The present state of the theory is embodied in the following expression for the mass excesses in MeV:

$$\Delta(^A\text{n}) = 104.7\ A^{-1} + 1.088\ A + 0.698\ A^{2/3} \quad (+\ 4.2 \text{ if } A \text{ is odd}),$$

$$\Delta(^A\text{H}_p),\ \Delta(^A\text{He}_p),\ \dots\ =\ \Delta(^A\text{n}) - 0.782\ Z + 0.57\ Z\ (Z-1)\ A^{-1/3} \tag{1}$$

where Z is the number of protons in the nucleus.

The following sections review the evidence supporting the mass excess formula and explore the extent to which the theory provides understanding of the new nuclear phenomena.

3. Chain reaction

High energy particles whose tracks are permanently recorded in CR39 detector chips provide irrefutable evidence for nuclear reactions and provide clues to the nature of the nuclear processes involved. One experiment in particular stands out in this regard. Oriani and I observed and analyzed a giant particle shower in the vapor over an active electrolysis system [16]. The electrolyte was a solution of lithium sulfate in ordinary water, and the cathode was nickel. A pair of opposing detector chips was hung in the vapor above the liquid surface. The shower contained about 150,000 alpha particles, of which about 30,000 were recorded on one detector chip and about 11,000 on the other. The particle energies were about 2 MeV indicting release of about 10^{-8} joules. Examination of the pattern of tracks indicates that the shower source was closer to the chip with 30,000 tracks than to the one with fewer tracks, and that it evolved rapidly before convection currents in the vapor carried it away. There was a very rapid initial portion that took place in a fraction of a second, followed by a slower portion that lasted for several seconds as the source moved along with the vapor.

Figure 1 is a photograph of the tracks recorded on one of nearly 300 areas that cover the surface of the 30,000-track chip. Figure 2 shows a plot of the variation of track density over the entire surface of the chip. The location of the initial rapid reaction is clearly visible at the large peak, as is the evolution of the slower reaction that drifts with convection currents. Theory must provide an explanation for these observations.

I assume that the particle shower in Figures 1 and 2 resulted from a polyneutron chain reaction that began with a single polyneutron in the vapor. (The source of this polyneutron is identified below.) Chain reaction requires that polyneutrons grow and divide in interaction with ordinary nuclei in a series of exothermic reactions, leading to exponential growth in their numbers. Potential fuels are limited to isotopes of hydrogen and oxygen present in the vapor. The isotopes ^{2}H (0.015%), ^{17}O (0.038%), and ^{18}O (0.200%) are among potential exothermic reactants because being more massive than their sibling isotopes ^{1}H and ^{16}O they can provide the required reaction energies. Their isotopic percentages are shown in parentheses.
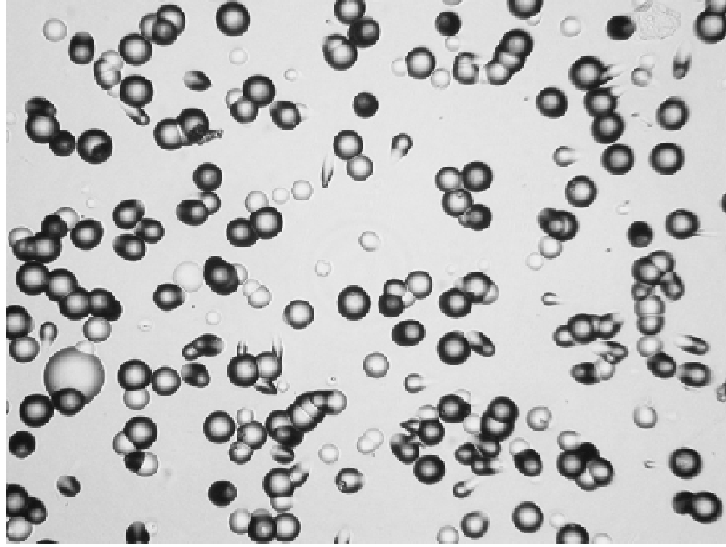
Figure 1. Etch pits on the surface of a CR39 plastic detector chip suspended in the vapor over an active electrolysis cell. Each pit marks the location of a track of damaged material where a charged particle has penetrated the chip. A roughly conical pit has developed during etching because the etchant attacks the damaged material of the track more rapidly than it attacks the adjacent undamaged material. The area shown measures approximately 0.58mm x 0.44mm. The mean diameters of the darker circular pits are approximately 24 microns.

Consider ^{2}H as a fuel. The known mass excesses $\Delta(^2H) = 13.136$ MeV and $\Delta(^1H) = 7.289$ MeV together with the polyneutron mass excesses from Formula 1 lead to the polyneutron growth reaction

$$^2H + {}^An \rightarrow {}^1H + {}^{A+1}n + (0.504/8.905) \text{ (even A/odd A), } (A \approx 600). \tag{2}$$
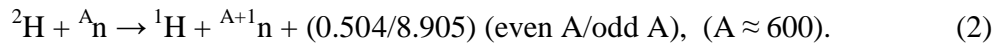
(Reaction energy values are always given in MeV.) The size of the polyneutron is not critical; for $A \approx 50$ the energy release changes only slightly to (0.474/8.873).
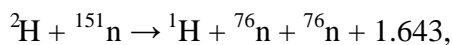
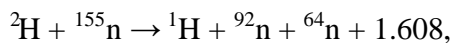Polyneutron fission reactions are exothermic with energy E for a range of odd A values,

$$^2H + {}^An \rightarrow {}^1H + {}^Bn + {}^{A-B+1}n + E \quad (49 \leq \text{odd A} \leq 1235, \text{ even B}). \tag{3}$$
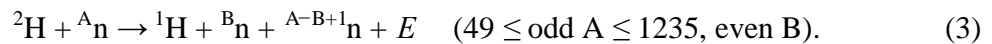
The energy E depends on the value of B. I assume that the most likely value of B is that for which E is a maximum. Examples of the most likely fissions for selected values of A include the smallest polyneutron that can undergo fission

$$^2H + {}^{49}n \rightarrow {}^1H + {}^{26}n + {}^{24}n + 0.119,$$
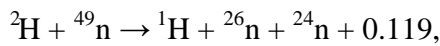
the largest polyneutron that fissions into equal parts

$$^2H + {}^{151}n \rightarrow {}^1H + {}^{76}n + {}^{76}n + 1.643,$$

and larger polyneutrons that fission into unequal parts

$$^2H + {}^{155}n \rightarrow {}^1H + {}^{92}n + {}^{64}n + 1.608,$$

$$^2H + {}^{299}n \rightarrow {}^1H + {}^{260}n + {}^{32}n + 0.369,$$
$$^2H + {}^{1235}n \rightarrow {}^1H \quad {}^{1204}n + {}^{32}n + 0.000.$$
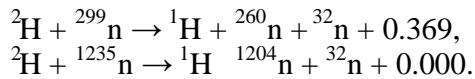
Reaction 3 completes a chain reaction in which many repetitions of reaction (2) cause a polyneutron to grow substantially, after which reaction (3) causes it to fission. Then the same series of reactions causes the fission products to grow and fission, and so on, providing the elements for exponential polyneutron multiplication and a runaway chain reaction.
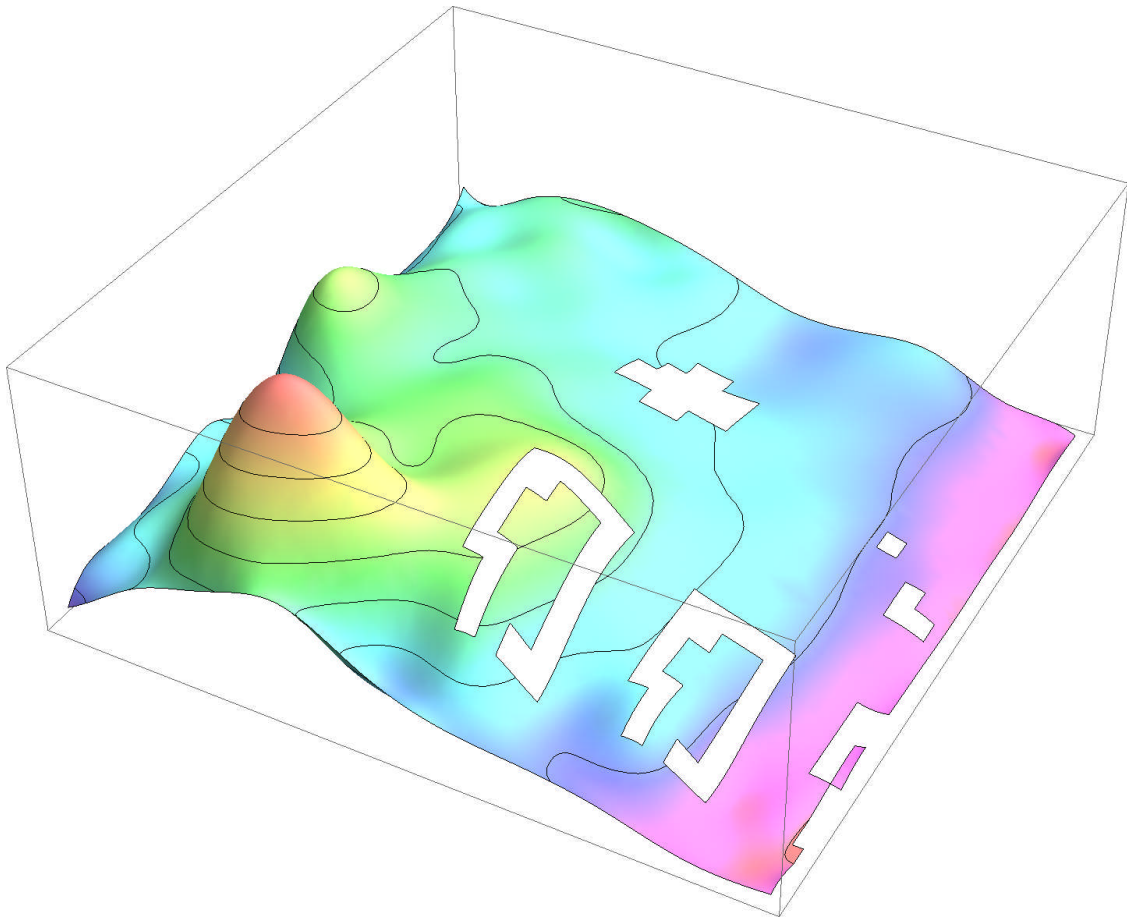

Figure 2. Density of tracks on the surface of a CR39 plastic detector chip suspended in the vapor over an active electrolysis cell. The chip area is about 0.64 cm^2 and the mean track density is about 45,000 cm^{-2}. White areas are areas where tracks could not be counted, including the hole for the supporting wire (cross shape at the top of the chip), factory-inscribed identifying numbers (bottom right of the chip), and a few areas with surface damage. The location of the initial reaction is clearly visible at the large peak, as is the evolution of the slower reaction that drifts with convection currents. Re-plotted from [16].

Yet the reaction in the shower experiment stopped before there was an explosion. Additional reactions must be considered. The hydrogen isotope ^1H cannot participate in neutron-transfer reactions with polyneutrons because all such reactions are endothermic. In consequence a ^1H nucleus and a polyneutron will maintain their unique identities even if they touch, and even if they bind through surface effects to form a composite nucleus. Evidence presented below suggests that nuclear composites play significant roles in polyneutron reactions. The composite that results from a polyneutron binding to ^1H is written $^1H^An$. Its components are written adjacent

to each other in analogy with chemical molecules such as NaCl. Composites can be formed in the reactions

$$^2H + {}^An \rightarrow {}^1H{}^Bn + {}^{A-B+1}n + E + E_b \quad \text{(odd A, even B)} \quad (4)$$
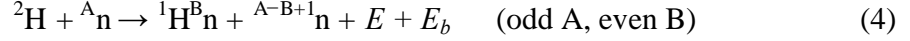
very similar to reaction (3) but where the reaction products ^1H and ^Bn form a composite with binding energy E_b. (I assume ^Bn to be the larger of the two product polyneutrons because I expect it to be more strongly bound to ^1H.)

Polyneutrons can interact with composites in reactions of the form

$$^1H{}^Bn + {}^An \rightarrow {}^1H{}^{B+A-C}n + {}^Cn + E \quad \text{(A+B} \geq 49\text{)}. \quad (5)$$
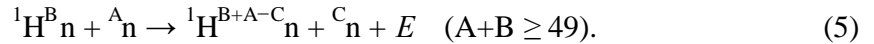
As a polyneutron grows larger through successive reactions (2) the free polyneutron ^Cn in reaction (5) grows smaller and reaches ^{32}n for very large composites. Reaction (3) shows that it must grow at least to ^{49}n before it can fission, requiring as many as 17 successive growth reactions (2). When the concentration of large composites is large enough, a single reaction (5) will return a free polyneutron to ^{32}n before the growth reactions have time to occur, in consequence of which all polyneutrons are reduced to sizes less than ^{49}n and kept there, the chain reaction stops, and the residual reactions involving small polyneutrons gradually die out as polyneutrons undergo beta decay, become charged, and can no longer participate in nuclear interactions.

We are left with the composites that were created in reaction (4) and that grew to large size by repetition of reaction (5). These composites are unstable and decay by coordinated beta decay and alpha particle emission. As shown below each composite emits many alpha particles, and together the alpha particles from decay of all composites constitute the giant shower shown in Figure 2.

4. Liquid drop model

In deriving the mass excess formula (1) I begin with a liquid drop model which in its simplest form is

$$\Delta(^An) = (\Delta(n) - a_v) A + a_s A^{2/3}.$$

In this expression the mass excess $\Delta(^An)$ equals the mass excess of A neutrons, less a volumetric term proportional to A that represents the strength of the nuclear binding energy of the drop, plus a term proportional to $A^{2/3}$ that represents the surface energy of the drop. Experimental evidence reviewed below requires that odd-A polyneutrons have an excess energy ε that must be included in the formula,

$$\Delta(^An) = (\Delta(n) - a_v) A + a_s A^{2/3} \quad (+ \varepsilon \text{ for odd A}).$$

The excess energy for odd A suggests that the neutrons in the droplet form a collective state with pair correlations similar to those in superconductivity where an odd electron has excess energy. Such correlations are long-range and extend over many neutrons. Let A_c be this correlation number. Then for $A < A_c$ the coefficients a_v and a_s are no longer constant but approach zero for

6

A = 4, where experiment [9] shows that $\Delta(^4\text{n}) \approx 4\,\Delta(\text{n})$. In an attempt to model the weakening of a_v and a_s for values of A less than the correlation number I introduce a term $a_0\,\text{A}^{-1}$ giving the final form of the polyneutron mass excess

$$\Delta(^A\text{n}) = a_0\,\text{A}^{-1} + (\Delta(\text{n}) - a_v)\,\text{A} + a_s\,\text{A}^{2/3} \ \ (+\,\varepsilon \text{ for odd A}).$$

In order to obtain numerical values for the four unknown parameters a_0, a_v, a_s, ε in this expression I require

1. $\Delta(^4\text{n}) = 4\,\Delta(\text{n})$ to agree with the marginal binding of ^{4}n,
2. Growth reaction (2) and tritium reaction (26) to be exothermic,
3. The isotope ^{150}Sm to be unreactive with large polyneutrons,
4. The parameter a_s to lie close to the maximum consistent with 1-3 above.

The first three requirements are objective but the fourth is subjective; smaller values of a_s are possible but seem less likely to me. The requirements are satisfied by parameters $a_v = 6.983$, $a_s = 0.698$, $a_0 = 104.7$, and $3.819 < \varepsilon < 4.704$. For definiteness I take $\varepsilon = 4.2$ in the middle of its range and arrive at the polyneutron mass excess in formula (1). The electrostatic terms in formula (1) are derived below.

5. Concerns

Mass excess formula (1) raises serious concerns. In particular the volumetric binding energy coefficient $a_v = 6.983$ is very large, amounting to 45% of the 15.5 value for ordinary nuclei [8]. This strong binding is in complete disagreement with calculations based on n-n reaction strengths derived from the energetics of ordinary nuclei, which predict that neutron aggregates are unbound. In addition the experimental observations that ^{2}n is unbound and that ^{4}n is at best marginally bound [9] do not hint at stronger binding for larger neutron aggregates. Yet strong binding is a requirement for the theory I propose; with weaker binding polyneutron growth cannot be exothermic and the theory collapses.

A second concern is the magnitude of the surface energy. In formula (1) the surface energy coefficient $a_s = 0.698$ is only 10% of the volumetric coefficient a_v. In contrast the value of $a_s = 16.8$ for ordinary nuclei is 108% of the volumetric coefficient. Yet small surface energy is another requirement for the theory; with larger surface energy polyneutron fission cannot be exothermic and the theory again collapses.

Rather than abandon the theory I note that the currently available n-n interaction strengths are phenomenological, not fundamental. They were designed to fit n-n interactions between neutrons that are constrained by the shell symmetry of ordinary nuclei. No interaction strengths have been published for aggregates of neutrons in mutual interaction free from shell model constraints. Mass excess formula (1) and supporting experimental evidence presented below suggest a cooperative neutron-pair interaction having symmetry related to electron pairing in superconductivity; one that does not reach full strength until the number of neutrons exceeds about 50. It then becomes possible to think that new interaction parameters apply. Then formula (1) can be viewed as a first step in determining the phenomenological interaction strengths for large clusters of neutrons. This is the spirit in which I proceed.

6. Correlation barrier

A significant feature of polyneutron reactions is the absence of neutrons among the reaction products. Neutron production cannot be ruled out by energetics. Consider polyneutron growth reaction (2),

$$^{2}H + {}^{A}n \rightarrow {}^{1}H + {}^{A+1}n + E_A \qquad (6)$$

which transfers a neutron from ^{2}H to polyneutron ^{A}n , promoting polyneutron growth and releasing energy E_A that depends only on the value of A. The related reaction

$$^{2}H + {}^{A}n \rightarrow n + {}^{A+1}H_p + E_A \qquad (7)$$

which transfers a proton to a polyneutron is also exothermic with exactly the same energy, but the near absence of neutrons in electrolysis experiments shows that it seldom occurs. Since it cannot be suppressed by energetics or by quantum selection rules I assume that it is kinetically inhibited by a potential barrier, similar in effect to the coulomb barrier which inhibits alpha decay.

Such a barrier can arise if the neutrons in a polyneutron participate in a collective condensation of pairs analogous to the electron-pair condensation in superconductivity. In this case a barrier is associated with the initial localization of the proton from ^{2}H as it merges into ^{A}n to form $^{A+1}H_p$. The wave function for the integrating proton corresponds initially to a localized proton at the surface of the polyneutron ^{A}n and finally to a distributed proton that is paired uniformly throughout $^{A+1}H_p$. In getting from the initial to the final configuration it has to pass through configurations where it is paired with a few neighboring neutrons and then with an increasing number of neutrons as it spreads out. The energy associated with pairing with only a few neutrons corresponds to the energies of $^{2}H_p$, $^{4}H_p$, $^{6}H_p$, and perhaps beyond, all of which are unbound or nearly so and have energies comparable to the same numbers of free nucleons. This is the correlation barrier that must be penetrated by a proton. In the present analysis I consider that reactions involving proton localization are strongly suppressed.

This is my justification for the assertion in Section 7 that alpha decay of polyneutron-derived nuclei is strongly suppressed: in these decays a correlation barrier must be overcome as distributed protons become localized to form ^{4}He. On the other hand there is no correlation barrier for beta decay because a distributed neutron transforms to a distributed proton without the necessity for localization.

By accepting the concept of a correlation barrier as necessary to suppress neutron generation, we must also accept collective neutron pairing and the consequence that an unpaired neutron does not share the binding energy of the fully paired state, leading to an excess energy for odd-A polyneutrons.

7. Polyneutron decay

Beta decay is the transformation of a neutron into a proton plus an electron plus an antineutrino. Reactions are often written with the proton and the electron combined in a

8

hydrogen atom and with the antineutrino implicit: n → ^{1}H. Following this practice I consider beta decay of a polyneutron that emits a free proton. This reaction is endothermic even for odd A and the maximum value of ε, and cannot occur spontaneously:

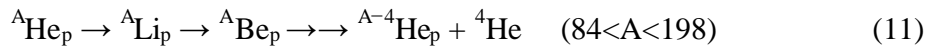$$^A n \rightarrow {}^{A-1}n + {}^1H - 5.088 \quad (\text{odd } A \approx 600). \tag{8}$$

Polyneutron beta decay can be exothermic only if the proton is incorporated into the transmuted polyneutron where it can participate in the nuclear symmetry, maintaining an unchanged nuclear interaction energy. Symbolically the transmuted polyneutron is ^AH_p, a massive hydrogen isotope that has the same paired spin structure as ^An, the same nuclear interaction energy as ^An, and the same excitation spectrum as ^An.

Let ^AZ_p represent any of the polyneutron-related nuclei ^An, ^AH_p, ^AHe_p, ^ALi_p, …, where Z reflects the number of protons in the nucleus. The liquid drop model for the mass excesses of ordinary nuclei contains the coulomb energy term $0.72\, Z\, (Z-1)\, A^{-1/3}$ [8]. Assuming that the densities of ^AZ_p are about half that of ordinary nuclei the coulomb contribution to their mass excesses is about $2^{-1/3}$ times as great. The overall mass excess for ^AZ_p then is

$$\Delta(^AZ_p) = \Delta(^An) - 0.782\, Z + 0.57\, Z\, (Z-1)\, A^{-1/3}. \tag{9}$$

This is the source of the electrostatic terms in formula (1). The $-0.782\, Z$ term is the energy associated with a loss of Z neutrons and a gain of Z protons and electrons.

Beta decay of polyneutron-related nuclei proceeds in the series of reactions $^An \rightarrow {}^AH_p \rightarrow {}^AHe_p \rightarrow {}^ALi_p \rightarrow {}^ABe_p \rightarrow {}^AB_p \rightarrow \ldots$ which continues until the buildup of coulomb energy from the increasing numbers of protons turns the reaction endothermic. Beta decay $^AZ_p \rightarrow {}^A(Z+1)_p$ is exothermic provided that $\Delta(^AZ_p)$ is greater than $\Delta(^A(Z+1)_p)$. If ^AZ_p is less than $^A(Z+1)_p$ beta decay is endothermic. However alpha decay of ^AZ_p is possible in the reaction $^AZ_p \rightarrow\rightarrow {}^{A-4}(Z-2)_p + {}^4He$ where a double arrow is used for alpha decays. In consequence we have several reaction chains, each corresponding to a distinct range of values of A, including

$$^ALi_p \rightarrow {}^ABe_p \rightarrow {}^AB_p \rightarrow\rightarrow {}^{A-4}Li_p + {}^4He \quad (198<A<388) \tag{10}$$

$$^AHe_p \rightarrow {}^ALi_p \rightarrow {}^ABe_p \rightarrow\rightarrow {}^{A-4}He_p + {}^4He \quad (84<A<198) \tag{11}$$

$$^AH_p \rightarrow {}^AHe_p \rightarrow {}^ALi_p \rightarrow\rightarrow {}^{A-4}H_p + {}^4He \quad (24<A<84). \tag{12}$$

A polyneutron with A in the range 198<A<388 undergoes successive beta decays until it reaches ^AB_p in reaction series (10). It then undergoes alpha decay to $^{A-4}Li_p$ which recycles in the same reaction chain through two beta decays and an alpha decay to $^{A-8}Li_p$ and so on losing four neutrons each cycle until the value of A drops below 198. The decay particle then cycles through reaction series (11) until A drops below 84, and then through series (12) until A drops below 24.

The half-life for alpha decay of polyneutron-related nuclei is expected to be much longer than the half-life for beta decay; alpha decay is slow because it must overcome the correlation barrier for distributed protons to localize in a helium nucleus (see section 6). Nuclei decay rapidly through the beta portions of chains (10-12) until they reach ^AB_p, ^ABe_p, or ^ALi_p, at which point they lie dormant awaiting the slower alpha decay. A dormant ^AB_p, ^ABe_p, or ^ALi_p that reaches the vapor will intermittently emit alpha particles as it cycles through successive iterations of reaction

chains (10-12). I suggest that these particles are responsible for the random scatter of tracks recorded on detectors in the vapor[13].

Reaction chains (11) and (12) cycle through $^A\text{He}_p$ which exceptionally can liberate a polyneutron in the slow alpha decay reaction

$$^A\text{He}_p \to\to {}^{A-4}\text{n} + {}^4\text{He} + 1.365 . \tag{13}$$

I suggest that this is the origin of the initial polyneutron that ignited a chain reaction in the vapor.

8. Particle showers

In addition to the giant shower pictured in figures 1 and 2 which contained about 150,000 alpha particles, Oriani and I have observed significantly smaller showers that contain at most a few hundred alpha particles [17]. I propose that both types of showers result from decay of $^{16}\text{O}^A\text{n}$ composites formed in reactions of polyneutrons with ^{17}O or ^{18}O such as

$$^{18}\text{O} + {}^B\text{n} \to {}^{16}\text{O}^A\text{n} + {}^{B-A+2}\text{n} \tag{14}$$

where $^{B-A+2}\text{n}$ is smaller than ^An. The related reaction in which both product polyneutrons are free is endothermic for all values of A and C. However reaction (14) can be exothermic provided that the binding energy E_b is sufficiently large. I assume this to be so.

In order to understand the decay of $^{16}\text{O}^A\text{n}$ it is desirable first to consider the role of polyneutron excitations in the decay of composite nuclei. I assume that polyneutrons have a spectrum of low-energy phonon-like excitation levels, and that partition of energy among these levels thermalizes in the strong-interaction time of about 10^{-20}s. These excitations can influence reaction rates on the same time scale because they are coupled by strong forces to other degrees of freedom in composites, and to reaction products as they are being formed. Partition between excitation and kinetic energies assures that polyneutrons absorb a portion of the energy released in every reaction in which they participate. I denote a hot polyneutron by $^A\text{n}^*$ and a hot composite by $^{16}\text{O}^A\text{n}^*$ and where desirable distinguish between hot and cold nuclei because they can have different reaction rates.

Turning now to consideration of $^{16}\text{O}^A\text{n}$ composite decay, beta decay that releases a free proton in the reaction $^{16}\text{O}^A\text{n} \to {}^{16}\text{O}^{A-1}\text{n} + {}^1\text{H}$ is endothermic and cannot occur. The reaction $^{16}\text{O}^A\text{n} \to {}^{16}\text{O}^A\text{H}_p$ is also endothermic because of the coulomb energy associated with the proximity of the proton in $^A\text{H}_p$ to the eight protons in ^{16}O. The composite also is stable against double beta decay $^{16}\text{O}^A\text{n} \to {}^{16}\text{O}^A\text{He}_p$ in which both protons of $^A\text{H}_p$ share the collective pair correlations with (A−2) neutrons. However exothermic decay can be accomplished by coordinated double beta decay and alpha particle emission. Decay of a cold composite is

$$^{16}\text{O}^A\text{n} \to\to {}^{16}\text{O}^{A-4}\text{n} + {}^4\text{He} + (2.147 - E_T) \tag{15}$$
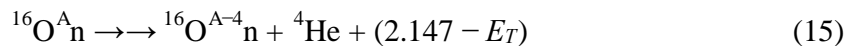
where E_T is the thermal energy of the hot product composite and $(2.147 - E_T)$ is the kinetic energy of the products. Decay of a hot composite is

$$^{16}O^An^* \rightarrow\rightarrow\ ^{16}O^{A-4}n^* + {}^4He + 2.147 \tag{16}$$
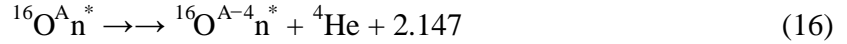
where the excitation of the reactant is passed on to the product. The half life of reaction (16) is shorter than for reaction (15) because more kinetic energy is available.

It is suggested below that large numbers of $^{16}O^An^*$ composites are formed in the vicinity of the cathode during electrolysis. I assume that some of them cool to $^{16}O^An$ by photon emission before they decay. Because reaction (15) is relatively slow some of these cold composites survive long enough to reach the vapor. When finally they decay the initial reaction (15) is followed by closely spaced multiple instances of reaction (16), releasing a small shower of particles. The giant shower shown in figures 1 and 2 can then be understood as the aggregate decays of hundreds of $^{16}O^An^*$ composites that were created in the chain reaction.
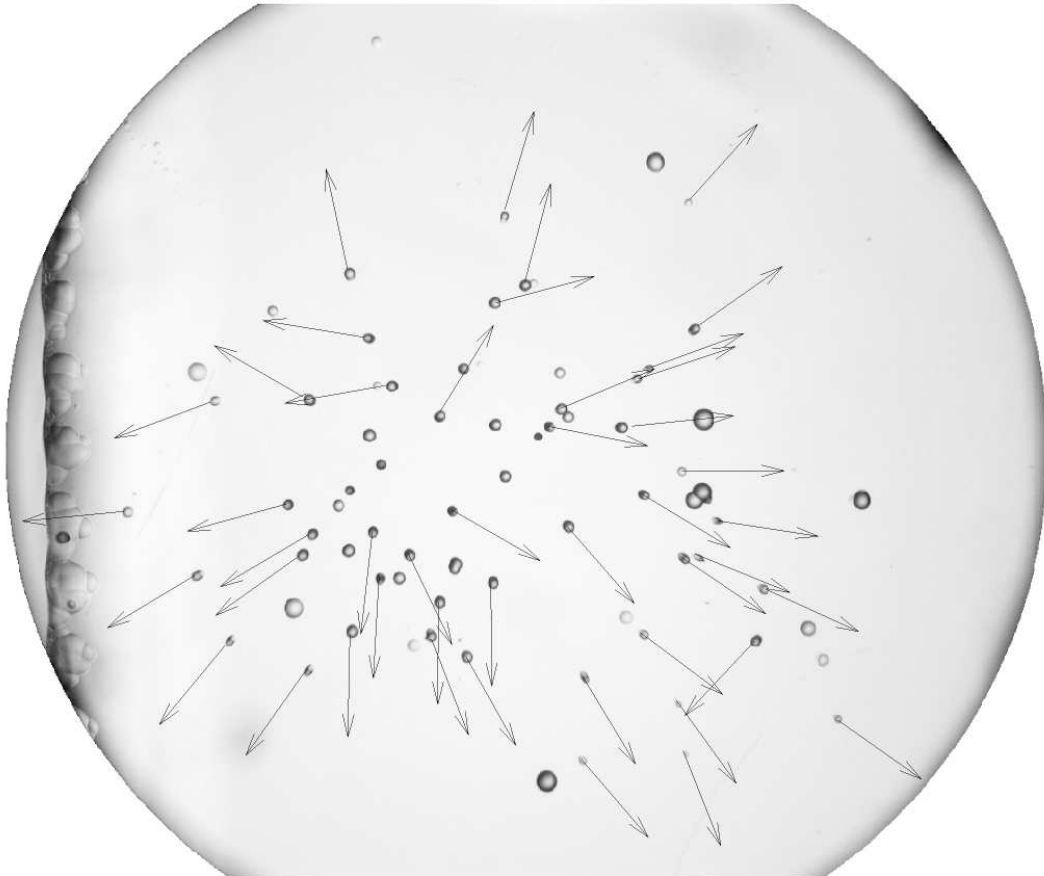

Figure 3. Shower of etch pits on a detector chip supported in air under a nickel cathode. The width of the image is approximately 2mm. Arrows indicate the directions in which charged particles impinged on the chip. The electrolyte was Li_2SO_4 in H_2O. (The virgin chip was etched before beginning the experiment to reveal pre-existing particle tracks. During the following etch they grew to twice the diameter of the experimental pits and can be distinguished by their large size.)

Figure 3 shows one of the small showers observed by Oriani [17]. In obtaining this shower he employed an electrolysis cell in which the electrolyte is contained within a vertically oriented glass tube and the cathode is a thin sheet of nickel that closes the bottom of the tube and provides

11

a watertight seal. The upper cathode surface is in contact with the electrolyte and the lower surface is in contact with air. The shower was recorded on a CR39 plastic detector placed in air under the cathode. To understand how this may have occurred I note that polyneutrons that enter the cathode from the electrolyte shrink in interactions with nickel. The most exothermic reaction involves ^{58}Ni (68%),

$$^{58}\text{Ni} + {}^{100}\text{n} \rightarrow {}^{62}\text{Ni} + {}^{96}\text{n} + 11.230. \tag{17}$$
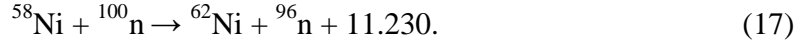
The reaction products share the energy, and that of product polyneutron ^{96}n exceeds 4 MeV. I assume that such energetic polyneutrons have relatively long mean free paths between repetitions of reaction (17) and that some of them penetrate the cathode and emerge into the air below it. Although polyneutrons in air can grow in interaction with ^{17}O in the reaction

$$^{17}\text{O} + {}^{101}\text{n} \rightarrow {}^{16}\text{O} + {}^{102}\text{n} + 11.230 \tag{18}$$
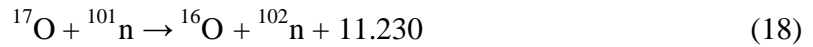
they also can shrink in interaction with ^{40}Ar in the reaction

$$^{40}\text{Ar} + {}^{101}\text{n} \rightarrow {}^{42}\text{Ar} + {}^{99}\text{n} + 1.739. \tag{19}$$
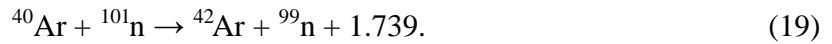
Because the concentration of ^{40}Ar in air is so large the shrinkage reaction overpowers the growth reaction and a chain reaction cannot be sustained. However formation of a composite $^{16}\text{O}^\text{A}\text{n}$ is possible by reaction (14), after which the composite can decay in a small shower by multiple instances of reaction (16) as described above. Each alpha emission in these reactions reduces the size of the polyneutron by four neutrons, in consequence of which the number of alphas emitted by a single composite is limited to 1/4 the number of neutrons in its initial polyneutron component. The 46 particle tracks recorded in figure (3) suggest about 150 alpha particles in the full shower and about 600 neutrons in the parent $^{16}\text{O}^\text{A}\text{n}$ composite. About 1000 such small showers together comprise the large shower in figure 2.

9. Role of electrolysis

In the foregoing we must identify the source of the $^{16}\text{O}^\text{A}\text{n}$ composites whose decays produce small showers of alpha particles in the vapor, and we must identify a source of polyneutron decay products $^\text{A}\text{B}_\text{p}$, $^\text{A}\text{Be}_\text{p}$, and $^\text{A}\text{Li}_\text{p}$ that release free polyneutrons in the vapor and ignite chain reactions. I propose that these precursors are formed in a region of extreme agitation near the cathode during electrolysis, and that a few are able to reach the vapor before they fully decay.

Hydrogen and deuterium atoms are generated at the cathode surface where they combine to produce molecules that supersaturate the electrolyte to a level that supports homogeneous bubble nucleation. Many tiny bubbles appear in the electrolyte near the cathode and trigger a maelstrom of competitive growth. Surface tension requires that bubbles of different sizes be in equilibrium with different levels of saturation, small bubbles with a high level and large bubbles with a lower level. At any given level bubbles larger than a critical size will grow and smaller bubbles will shrink. The situation is unstable. Minor differences in size and in local hydrogen or deuterium concentration enable a few bubbles to take the path of runaway growth while the majority shrink and vanish. Then growth of the large bubbles slows as they move away from the region of bubble nucleation.

12

Now consider the fate of a polyneutron in the electrolyte near the surface of a bubble in its rapid growth stage. There it ignites a chain reaction and the concentration of $^{16}O^An^*$ reaction products begins to rise. The cloud of reaction products that would have built up and would have quenched the reaction in a quiescent fluid gets stretched tangentially and shrunken radially into a portion of a thin spherical shell. The thickness of the active region tends to increase because of the continuing chain reaction but it is held in check by the thinning action of bubble expansion. Reaction can persist as long as bubble growth is rapid, but ultimately a bubble moves into a region with a lower concentration of dissolved gas and the growth rate slows. The thinning rate becomes insufficient to stop buildup of composite nuclei poisons and reaction at that bubble is quenched. But this is not the end of the story. The reaction from an active bubble can be transferred by polyneutron diffusion to rapidly growing bubbles behind it, igniting them, and the process can continue indefinitely with the result that a bounded reaction rate can be maintained near the surface of the cathode where bubble nucleation and rapid growth occur. In summary, a single polyneutron that is released near a rapidly growing bubble in an electrolysis experiment can ignite a reaction that will persist near the cathode as long as electrolysis persists, whereas in contrast a chain reaction in a quiescent electrolyte is quenched by localized buildup of poisons. In this interpretation fluid agitation is the key contribution of electrolysis.

I assume that other means than electrolysis, including mechanical agitation, can maintain the high fluid shear rate required to disperse poisons and to provide a steady input of fresh reactant for maintaining a reaction. In consequence I expect that here and there in rapidly flowing streams and waterfalls where sufficiently high shear rates exist, chain reactions are proceeding with ^2H from water as fuel, and are providing ongoing sources for ^AB_p, ^ABe_p, and ^ALi_p nuclei. Chemically these nuclei are massive boron, beryllium, and lithium isotopes that mix along with their decay products ^AH and ^AHe into the hydrosphere and the atmosphere, where further decay via reactions (10-13) provides free polyneutrons that can ignite new chain reactions in nature and in the laboratory.

10. Transmutation 1. Chain reaction.

The most careful and instructive studies of transmutation have been conducted by Iwamura and associates [5-7]. They designed an apparatus in which an element to be transmuted, the target element, was deposited on the front surface of a specially constructed palladium diaphragm containing in its interior thin layers of CaO. Deuterium was passed through the diaphragm from a pressurized chamber on the front side to a vacuum chamber on the back side. During each experiment concurrent X-ray photoelectron spectroscopy (XPS) showed that a new chemical element appeared on the surface where none had been before, and that the concentration of the target element declined.

I discuss first the mechanism by which a nuclear reaction can be sustained in this system. Because the deuterium gas is quiescent, the mechanism that maintains the reaction cannot be mechanical agitation as proposed for electrolysis experiments. I suggest a second mechanism in which calcium plays a key role. I assume that the chain reaction persists primarily in the deuterium gas where polyneutron growth can be sustained. Polyneutrons that enter the palladium shrink rapidly because shrinkage reactions are exothermic and growth reactions are endothermic. Nevertheless some polyneutrons survive to reach the CaO films where they can react with calcium. The major calcium isotope ^{40}Ca (97%) reacts vigorously with small polyneutrons in reactions such as

$$^{40}\text{Ca} + {}^{58}\text{n} \rightarrow {}^{48}\text{Ca} + {}^{50}\text{n} + 18.769. \tag{20}$$
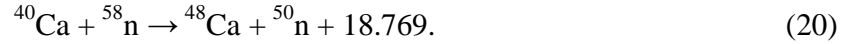
Polyneutrons composed of 50 or fewer neutrons exit reaction (20) with energies of 9 MeV or more. I assume that some of them penetrate back through the palladium film that lies between the CaO and the deuterium gas to where they ignite fresh volumes of deuterium that lie beyond the previously generated poisons ${}^{1}\text{H}^{A}\text{n}$ that are flowing into and through the palladium with the general current of hydrogen isotopes.

It has been shown that calcium is essential for maintaining the reaction [6]. No reaction occurred when MgO was substituted for CaO in the layered foil. This is consistent with theory. The major magnesium isotope ${}^{24}\text{Mg}$ (79%) reacts with small polyneutrons in reactions such as

$$^{24}\text{Mg} + {}^{54}\text{n} \rightarrow {}^{28}\text{Mg} + {}^{50}\text{n} + 5.781 \tag{21}$$
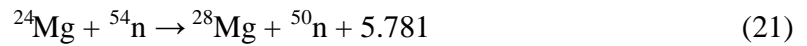
which produces polyneutrons with about a third of the energy of the calcium reaction. Few if any of these polyneutrons have sufficient energy to reach the deuterium gas before they thermalize and decay, and hence a chain reaction cannot be sustained when Mg is substituted for Ca.

10. Transmutation 2. Selected reactions.

The analysis in this section is based on the transmutation research of Iwamura *et al.* [5-7]. Their observations provide both qualitative and quantitative challenges to theory. Table 1 lists the transmutation reactions they have reported, together with additional reactions that have been deduced from their published results. The table also provides interpretations that are discussed in more detail below.

The transmutations

$$
\begin{aligned}
\text{Sr} &\rightarrow \text{Mo} & \Delta Z &= 4 \\
\text{Cs} &\rightarrow \text{Pr} & \Delta Z &= 4 \\
\text{Ba} &\rightarrow \text{Sm} & \Delta Z &= 6
\end{aligned}
\tag{22}
$$

were studied by several techniques and are firmly established. To good approximation the increase of Mo nuclei occurs simultaneously with the decrease of Sr nuclei as detected by X-ray photospectroscopy. Similarly the increase of Pr occurs simultaneously with the decrease of Cs as does the increase of Sm with the decrease of Ba. This strongly suggests that these transmutations do not proceed through intermediate steps of comparable duration, but in closely bunched multiple steps that lead to relatively long-lived isotopes that build up in concentration and reveal themselves as transmutation products.

TABLE 1

Transmutations of Sr, Cs, and Ba targets on a Pd substrate. Column 1 lists target elements and isotopes with references to the experiments. Column 2 lists the corresponding chemical signals observed for the transmuted elements. XPS stands for X-ray photoelectron spectroscopy and XRF for X-ray fluorescence spectroscopy. XPS signals are identified by the photoelectron energy levels employed for element identification. Column 3 lists the relative strengths of XPS signals observed. Column 4 lists mass numbers determined by secondary ion mass spectrometry (SIMS). The final column provides interpretations of the experimental observations. Interpretations based on polyneutron theory are found in references 1, 20, 21, and 22.

Target	Experimental Signal	Strength	Mass No.	Interpretation
Sr [5]	XPS: Mo3d5, Mo3d3	$--$	96	$^{88}Sr \rightarrow {}^{96}Mo$ [5]
				$^{88}Sr \rightarrow {}^{96}Zr + {}^{100}Mo$ [1]
Cs [5]	XPS: Pr3d5, Pr3d3	$--$	141	$^{133}Cs \rightarrow {}^{141}Pr$ [5,1]
Cs [7]	XRF: La, Ba, or Ti	$--$	$--$	$Cs \rightarrow La$, Ba, or Ti [7]
				$Cs \rightarrow La$ or Ba [1]
Ba [6]	XPS: Sm3d5, Sm3d3	9,6	$--$	$^{138}Ba \rightarrow {}^{150}Sm$ [6,1]
Ba [6]	XPS: Nd3d5, Nd3d3	4, 1	$--$	$^{138}Ba \rightarrow {}^{144}Nd$ [20]
Ba [6]	XPS: Xe3d5, Xe3d3	2, ½	$--$	$^{137}Ba \rightarrow {}^{136}Xe$ [21]
^{137}Ba [6]	$-$	$--$	138	$^{137}Ba \rightarrow {}^{138}Ba$ [22]

It also suggests that transmutation reactions occur within composite nuclei that form in the initial polyneutron reaction with a target nucleus. Then each further step can proceed rapidly without having to wait for a new polyneutron. I assume that catalyzed beta decay can drastically shorten lifetimes and allow rapid sequential beta decays within the composite nuclei $^{88}Sr^A$n, $^{133}Cs^A$n, and $^{138}Ba^A$n. One's imagination is stretched to contemplate that a weak reaction such as beta decay, with a half-life that can exceed many years for a free nucleus, can be catalyzed to a half-life on order of days, or perhaps seconds or less in a nucleus/polyneutron composite. Yet I see no other way that polyneutron theory can account for the experimental results, and I proceed on the assumption that such catalysis does occur. Perhaps it comes about because of an ability of polyneutrons to absorb energy in a spectrum of low-energy excitations on a nuclear timescale. This is a much shorter time scale than that for free beta decay and would allow a polyneutron to absorb much of the reaction energy, speeding the process and leaving a smaller proportion of energy for the emitted electron and neutrino. In turn this would diminish the energy of bremsstrahlung from the emitted electron, in agreement with the failure to detect energetic bremsstrahlung in transmutation experiments. X-rays emitted as the polyneutron cooled would also agree qualitatively with the observation of X-rays in the transmutation experiments [4].
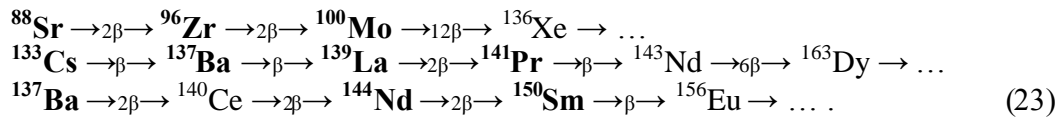
The concentration of even polyneutrons in a chain reaction is expected to be much greater than that of odd ones. This follows from reaction (2) where reaction of an odd polyneutron with ^{2}H is exothermic by 8.905 MeV and the reaction of an even polyneutron to produce an odd one is exothermic by only 0.504 MeV. Odd polyneutrons are converted rapidly to even ones, which only slowly are converted to odd ones. Steady state corresponds to a preponderance of even

polyneutrons. Because more of them are available I expect that most transmutation reactions will be initiated by even polyneutrons, and I temporarily neglect odd ones.

With the foregoing assumptions, transformation of a nucleus of ^{88}Sr, ^{133}Cs, or ^{138}Ba begins with formation of a nucleus-polyneutron composite. Within the composite neutrons flow from the polyneutron to the nucleus until the composite reaches its minimum energy. Beta decay then follows (or double beta decay if single beta decay is endothermic) and neutrons flow again until the transmuted composite reaches its minimum energy. We have a series of beta decays, each accompanied by an equilibrating flow of neutrons. The mass number of a nucleus grows as neutrons are added to it, but the mass number of the composite remains unchanged. I assume that beta decay of a nucleus in a composite is catalyzed by the polyneutron and occurs in a short time regardless of its lifetime as a free nucleus. Note in particular that some nuclei that are stable when free can undergo beta decay when bound in composites because of the associated flow of neutrons that can occur.

A transmuted composite can dissociate into a free transmuted nucleus and a free polyneutron provided that the reaction is exothermic. At any given time some transmuted nuclei remain bound in composites and some have been freed. Chemically and physically a composite such as ^{138}Ba^{600}n is a barium isotope with mass number 738. X-ray photospectroscopy (XPS), which measures electronic energy levels, will identify both free nuclei and composites as barium. Secondary ion mass spectroscopy (SIMS), which measures mass, can identify only free nuclei. I assume that beta decay of bound nuclei that are stable when free is slower than decay of nuclei that are unstable when free. In consequence only stable nuclei survive long enough to accumulate in sufficient numbers to become observable by either XPS or SIMS.

The first few isotopes in the theoretical transmutation chains for ^{88}Sr, ^{133}Cs, and ^{138}Ba that are stable when free, and that are expected to accumulate to an observable concentration, are

$$^{88}\textbf{Sr} \rightarrow_{2\beta}\rightarrow {}^{96}\textbf{Zr} \rightarrow_{2\beta}\rightarrow {}^{100}\textbf{Mo} \rightarrow_{12\beta}\rightarrow {}^{136}\text{Xe} \rightarrow \dots$$
$$^{133}\textbf{Cs} \rightarrow_{\beta}\rightarrow {}^{137}\textbf{Ba} \rightarrow_{\beta}\rightarrow {}^{139}\textbf{La} \rightarrow_{2\beta}\rightarrow {}^{141}\textbf{Pr} \rightarrow_{\beta}\rightarrow {}^{143}\text{Nd} \rightarrow_{6\beta}\rightarrow {}^{163}\text{Dy} \rightarrow \dots$$
$$^{137}\textbf{Ba} \rightarrow_{2\beta}\rightarrow {}^{140}\text{Ce} \rightarrow_{2\beta}\rightarrow {}^{144}\textbf{Nd} \rightarrow_{2\beta}\rightarrow {}^{150}\textbf{Sm} \rightarrow_{\beta}\rightarrow {}^{156}\text{Eu} \rightarrow \dots \, . \qquad (23)$$
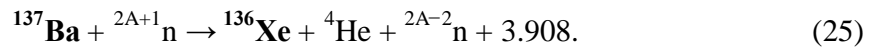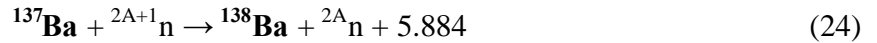
The numbers of intermediate beta decays between stable (when free) nuclei are indicated in the arrows.

The parameters of the polyneutron mass excess $\Delta(^A\text{n})$ were selected to assure that ^{150}Sm is stable with respect to neutron transfers to or from a large polyneutron. This provides the tight constraint described in requirement 3 of Section 4 and leads to the chains of stable isotopes (23) that are inert to neutron transfers. The transmutation products listed in Table 1 are shown in bold face type in the transmutation chains. Every observed transmutation product is contained within these chains, and they tend to be the products that require the smallest numbers of beta decays. At present the theory is not capable of determining the rates of the steps in the various reaction chains, and cannot predict which products will accumulate to an extent that they can be detected.

Experimental evidence for strontium transmutation consists of an XPS signal for molybdenum and a SIMS signal for mass 96. It is natural to suggest ^{96}Mo as the transmutation product. However the theory identifies the XPS signal with ^{100}Mo and the SIMS signal with ^{96}Zr. If ^{96}Zr were present one would expect an XPS signal for Zr; however this signal falls on top of the signal for the Pd substrate and would be undetectable if present. If ^{100}Mo were present one would

expect a SIMS signal at mass 100, but the experimental SIMS measurement shows little if any enhancement at mass 100, suggesting that most ^{100}Mo is bound in composites leaving only a low concentration of free ^{100}Mo. Theory does not yet provide means for determining the fraction of transmuted nuclei that have been freed. If further research should rule out ^{100}Mo as a transmutation product, the theory would have to be modified to include additional stable nuclei as transmutation products.

Reactions involving transfer of a single neutron can involve transmutation of a target nucleus into a free product, or into the initial composite of a reaction chain. Two reactions with free product nuclei are

$$^{137}\text{Ba} + {}^{2A+1}\text{n} \rightarrow {}^{138}\text{Ba} + {}^{2A}\text{n} + 5.884 \tag{24}$$

$$^{137}\text{Ba} + {}^{2A+1}\text{n} \rightarrow {}^{136}\text{Xe} + {}^{4}\text{He} + {}^{2A-2}\text{n} + 3.908. \tag{25}$$

These reactions are both exothermic with comparable energy release, and there is experimental evidence for both as indicated in Table 1.
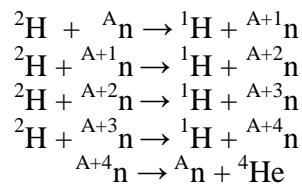
12. Deuterium reactions

Experiment suggests that deuterium plays a role in energy generation and in tritium production. These reactions provide bounds on the value of the excess energy ε associated with an odd neutron in an interacting polyneutron. For energy generation we must have a chain reaction, and the polyneutron growth reactions must be exothermic. The polyneutron growth reaction (2) requires $\varepsilon < 4.708$ MeV. For tritium production we must have the exothermic reaction

$$^{2}\text{H} + {}^{2A+1}\text{n} \rightarrow {}^{3}\text{H} + {}^{2A}\text{n} + (\varepsilon - 0.671) \tag{26}$$
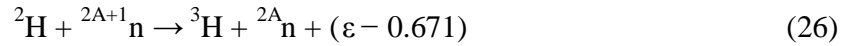
which requires $\varepsilon > 0.671$ MeV. These exothermic requirements provide constraints on the value of ε in mass formula (1).

The maximum rates of energy evolution during electrolysis have been obtained using heavy water D_2O for the electrolyte and palladium for the cathode. During electrolysis the cathode absorbs large quantities of deuterium, amounting to nearly one deuterium atom per palladium atom. Under these circumstances a deuterium chain reaction can proceed within the cathode free of competition from oxygen and lithium fuels in the electrolyte, but subject to transmutation reactions between polyneutrons and palladium isotopes. I assume that the primary energy-producing reactions are polyneutron growth and decay. The sequential reactions

$$^{2}\text{H} + {}^{A}\text{n} \rightarrow {}^{1}\text{H} + {}^{A+1}\text{n}$$
$$^{2}\text{H} + {}^{A+1}\text{n} \rightarrow {}^{1}\text{H} + {}^{A+2}\text{n}$$
$$^{2}\text{H} + {}^{A+2}\text{n} \rightarrow {}^{1}\text{H} + {}^{A+3}\text{n}$$
$$^{2}\text{H} + {}^{A+3}\text{n} \rightarrow {}^{1}\text{H} + {}^{A+4}\text{n}$$
$$^{A+4}\text{n} \rightarrow {}^{A}\text{n} + {}^{4}\text{He}$$

lead to the overall reaction

$$4(^2H) \rightarrow 4(^1H) + {}^4He + 21. \tag{27}$$

(Note that the polyneutron reactants are identical to the polyneutron products and they cancel each other out.) This energy value is approximate. Neglected palladium transmutation reactions produce less helium per unit of energy released, and neglected chain reactions in the electrolyte produce more helium per unit energy. Overall I conclude that 21 MeV per helium atom is an approximate value for reactions between polyneutrons and deuterium within a palladium cathode. This can be compared with the experimental value of approximately 24 MeV per helium atom [3].

13. Assessment

Polyneutron theory offers natural explanations for many of the new low-temperature phenomena found to date, including large alpha particle showers in the vapor over an electrolyte, small alpha showers in the vapor, alpha particles in the electrolyte and in the air beyond, nuclear energy generation, transmutation, helium production and tritium production. Although the range of experiments available for verifying consistency of the theory is limited, a few cross-checks are possible. Theory suggested early on that energetic alpha particles could be detected in the vapor of an active electrolysis cell and in the air outside the cell, as subsequently verified by particle shower experiments. The mass formula, derived by fitting the theory to samarium and tritium reactions, implies an energy of 2.1 MeV for shower particles in agreement with the experimental value of 2 MeV. It also accounts for the positive role of calcium and the negative role of magnesium in supporting reactions in transmutation experiments. It suggests previously unrecognized transmutations for which evidence has been found in published experimental results. The theory also suggests energy and helium generation in the ratio of about 21 MeV per helium atom in palladium, in reasonable agreement with the experimental value of about 24 MeV.

We have here only a beginning toward reaching the level of quantification that has been achieved in neutron physics, but it is a beginning that I believe holds the seeds of true understanding of the nascent field of polyneutron physics.

14. Acknowledgements

15. Bibliography

1. J. C. Fisher, interpretation in this paper.
2. M. Fleischmann, S. Pons, and M. Hawkins, *J. Electroanal. Chem.* **261**, 301 (1989) and erratum **263**, 187 (1989).
3. P. L. Hagelstein, M. C. H. McKubre, D. J. Nagel, T. A. Chubb and R. J. Heckman, *Proc. 11th Intl. Conf. Cold* Fusion, Marseilles, France, 31 Oct.−5 Nov. 23 (2004).
4. Y. Iwamura, T. Itoh and M. Sakano, *Proc. 7th Intl. Conf. Cold Fusion*, Vancouver, Canada, 19−24 April, 167 (1998).
5. Y. Iwamura, M. Sakano and T. Itoh, *Jpn. J. Appl. Phys.* **41,** 4672-4650 (2002).
6. Y. Iwamura, T. Itoh, M. Sakano, N. Yamazaki, S. Kuribayashi, Y. Terada, T. Ishikawa and J. Kasagi, *Proc 11th Intl. Conf. Cold Fusion*, Marseilles, France, 31 Oct.−5 Nov. 339 (2004).
7. Y. Iwamura, T. Itoh, M. Sakano, N. Yamazaki, S. Kuribayashi, Y. Terada and T. Ishikawa, *Proc. 12th Intl. Conf. Cold Fusion*, Yokohama, Japan, 27 Nov.−2 Dec. 178 (2005).
8. K. S. Krane, Introductory Nuclear Physics, John Wiley & sons, New York, 1988, p. 68.
9. F. M. Marques, M. Labiche, N. A. Orr, *Phys. Rev. C* **65,** 044006 (2002).
10. M. C. H. McKubre, S. Crouch-Baker, R. C. Rocha-Filho, S. I Smedley, F. L. Tanzenelle, T. O. Passel, and J. Santucci, *J. Electroanal. Chem.* **368**, 55 (1994).
11. M. H. Miles, B. F. Bush, G. S. Ostrom, and J. J. Lagowski, *Fusion Technology* **25**, 478 (1994).
12. R. A. Oriani, J. C. Nelson, S. Lee, and J. H. Broadhurst, *Fusion Technology* **18**, 652 (1990).
13. R. A. Oriani and J. C. Fisher, *Jpn. J. Appl. Phys.* **41**, 6180 (2003) and erratum **42**, 1498 (2003).
14. R. A. Oriani and J. C. Fisher, *Trans. Am. Nuc. Soc.* **88**, 640 (2003).
15. R. A. Oriani and J. C. Fisher, *Proc. 10th Intl. Conf. Cold Fusion*, Cambridge, Mass., 24−29 Aug. 567 (2003).
16. R. A. Oriani and J. C. Fisher, *Proc. 11th Intl. Conf. Cold Fusion, Marseilles, France*, 31 Oct.−5 Nov. 281 (2004).
17. R. A. Oriani and J. C. Fisher, *Proc. 11th Intl. Conf. Cold Fusion, Marseilles, France*, 31 Oct.−5 Nov. 295 (2004).
18. E. K. Storms, The Science of Low Energy Nuclear Reactions: A comprehensive compilation of evidence and explanations about cold fusion, World Scientific, 2007.
19. F. G. Will, K. Cedzyuska, and D. C. Linton, *Proc. 4th intl. Conf. Cold Fusion,* Lahaine, Maui, 6−9 Dec. (1993).
20. Based on full XPS energy spectrum for barium transmutation [6]. A clear Nd signal can be seen.
21. Based on full XPS energy spectrum for barium transmutation [6]. A signal for Xe can be seen after subtracting a small overlapping Pd signal.
22. Based on SIMS data for ^{137}Ba transmutation, adjusted for probable carbon contamination of the ^{137}Ba measurement.